OWC channel measurement testbed building in indoor environment with m-CAP modulation

Ziqi Liu, Xun Zhang, Bastien Béchadergue

2023 IEEE International Symposium on Broadband Multimedia Systems and Broadcasting (BMSB) | 979-8-3503-2152-4/23/$31.00 ©2023 IEEE | DOI: 10.1109/BMSB58369.2023.10211245

OWC channel measurement testbed building in indoor environment with m-CAP modulation

1st Ziqi LIU
LISITE-ECoS
Institut supérieur d'électronique de Paris
Paris, France
ziqi.liu@isep.fr

2nd Xun ZHANG* (IEEE senior member)
LISITE-ECoS
Institut supérieur d'électronique de Paris
Paris, France
xun.zhang@isep.fr

3rd Bastien Béchadergue
LISV
Université de Versailles Saint-Quentin
Vélizy-Villacoublay, France
bastien.bechadergue@uvsq.fr

***Abstract*—In recent years, with the rapid deployment of 5G and the planning for future 6G multi-network convergence, interest in optical wireless communication (OWC) technology as a promising complementary technology to Radio Frequency (RF) technology has gained new impetus. In this paper, aiming at the OWC communication system, an indoor OWC channel measurement testbed is built to measure the infrared (IR) channel under the testbed and evaluate its communication performance. Through experiments, the channel response of the IR device is measured. The OWC channel measurement testbed can achieve a data rate above 16Mbps, with the minimum value of Error Vector Magnitude (EVM) 18.8338%, and the minimum value of Bit Error Ratio (BER) 0.0301. According to the Digital Cinema System Specification (DCSS) issued by Digital Cinema Initiatives (DCI), the system meets the transmission standard of 4K radio.**

***Index Terms*—OWC, channel measurement, m-CAP, IR, access point (AP)**

I. Introduction

With the rapid commercialization of 5G around the world, the society will not only be better connected, through the enhancement of communication capabilities such as higher speed and lower latency, but also, more devices such as automobiles, buildings, and even home appliances [1]. With the deployment of 5G, the transition from a connected society to connected everything, and the next generation of mobile communication network 6G is expected to provide a platform called "Intelligent Connection of Everything" [2]. Under the 6G network architecture, there are more potential applications such as smart home, intelligent medical care, smart city, and the Internet of Vehicles [3], sensing (i.e. detecting and responding to some type of input from the physical environment) is not only an independent function, but also more tightly integrated with communication. The emergence of integrated sensing and communication (ISAC) provides a gain in the performance of communication and sensing [4]. But 6G is expected to deliver 100 times faster access speeds and 1000 times capacity than 5G to support the explosive growth of bandwidth demand [5]. To this end, all spectra including optical frequency bands will be fully explored to further have the advantages of wide bandwidth for both communication and sensing [5]. Based on the above factors, ISAC in the optical frequency bands or higher-frequency bands has become a key technology in the future 6G architecture.

Compared with traditional radio frequency-based ISAC systems, the signal bandwidth is strictly limited and the frequency band is almost exhausted, ISAC systems based on optical wireless communication (OWC) have more advantages, such as high bandwidth, high security, low power consumption, low infrastructure and equipment costs, and non-interference with RF devices and networks [6]. network switch In addition, the ISAC system based on OWC is a supplement to the existing radio frequency wireless network, meets the needs of future heterogeneous networks and hybrid networks, and realizes the goal of 6G multi-network integration [6].

OWC has emerged as a promising green, secure, and interference-free alternative complement to existing Radio Frequency (RF) communication technologies for next-generation communication systems [7]. Despite the growing literature about OWC and infrared (IR) communication, there is still a lack of work on indoor channel measurements and communication testing. This is a serious issue because this work not only sheds light on the link design and specifies the fundamental constraints of the physical layer design of OWC systems, i.e. transmit power and receiver complexity, but also verifies its communication performance.

For the indoor testing of OWC, not only the channel needs to be measured, but also its communication performance should be the key object of investigation. The severe bandwidth limitation of the OWC transmission equipment is the main bottleneck of high-capacity OWC [8]. The most commonly proposed technique to increase the OWC data rate is to use a modulation format with high spectral efficiency, such as Orthogonal Frequency Division Multiplexing (OFDM) [9]. Recently, research activity on OFDM for OWC has decreased, as multi-band carrierless amplitude and phase modulation (m-CAP) has been shown to outperform OFDM over the same experimental links [10]. In m-CAP, the carrier frequency is generated using a finite impulse response filter, which is cost-effective and easily reconfigurable, and greatly reduces computational complexity compared to OFDM systems that require (inverse) fast Fourier transforms [11]. Meanwhile, m-CAP has also been shown to be an effective method for improving OWC bandwidth utilization [12].

In this paper, we built an indoor OWC testbed, and used it to measure the OWC channel parameters in an IR band centered on 940 nm. Then, we used this testbed to evaluate the communication performance when using an m-CAP modulation scheme.

The remainder of this paper is organized as following: the section II proposes a scheme to build an indoor channel testbed based on OWC. The section III presents the construction and operation. The section IV presents the result analysis of the experimental environment. The discussion and conclusion are presented in the section V.

II. OWC System Model and m-CAP Modulation

This section introduces the OWC system model and application scenarios, as well as the m-CAP modulation method scheme chosen to test the communication functions.

A. System Model

To realize the OWC function indoors, after receiving the information to be transmitted from an external cloud or server, visible or IR Light-Emitting Diodes (LEDs) are used as the access points to transmit the signal. Among them, while the LEDs complete the communication function, the original lighting function is not affected. At the receiving end, photodiodes (PDs) are used as receiving devices, to receive the optical wireless signal, which may be received by different types of users.

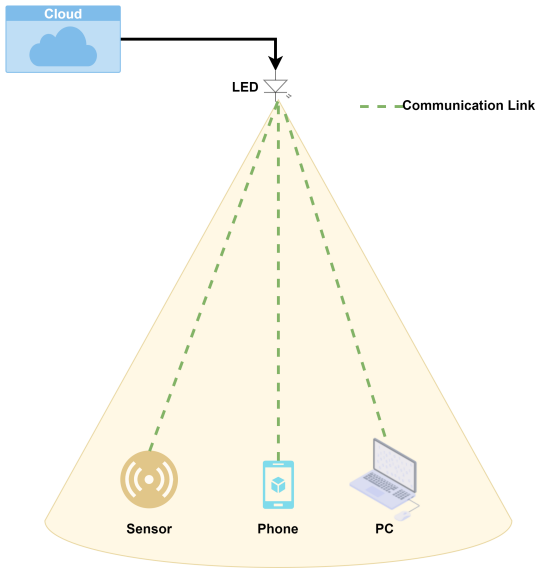

Fig. 1. Indoor OWC System usage scenario diagram

In the indoor OWC test bench to be built, IR emiters and LEDs will be used as transmission access points, and OWC channels (IR channels or visible light communication (VLC) channels) are used to communicate, so that devices at the receiving end, such as sensors, mobile phones, laptops, and other terminal devices, can obtain the signal to realize the indoor communication function. The usage scenario diagram of indoor OWC System is shown in Fig.1.

B. m-CAP Modulation

In order to realize the detection of the communication performance of the OWC system indoors, m-CAP modulation is selected as the signal modulation. CAP is essentially a different implementation of the traditional Quadrature Amplitude Modulation (QAM), with similar performance [13]. m-CAP transforms the traditional CAP into a multi-carrier format. The spectrum is divided into multiple subcarriers, each using a CAP modulation process with a pair of Hilbert pulse-shaping filters of the center frequency corresponding to that subband [14] (the m-CAP modulation and demodulation process is shown in Fig.2). It reduces the susceptibility to non-flat channel response in conventional CAP and increases scheme flexibility by allowing the use of bit and power loading techniques [15].

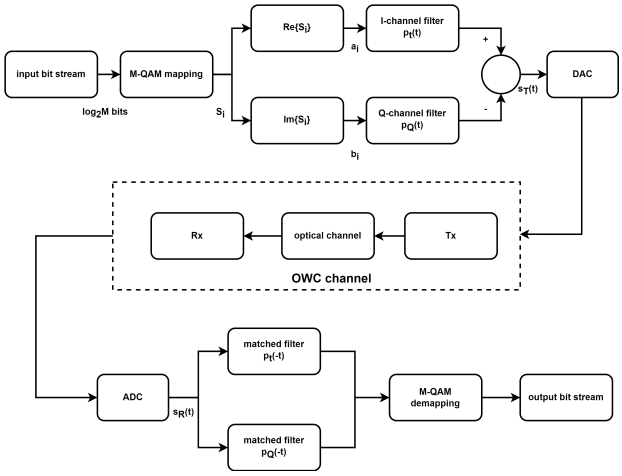

Fig. 2. m-CAP modulation and demodulation flowchart

In order to provide a low-complexity way to obtain high data rate and high multi-user capacity, m-CAP is selected as the modulation method. Compared with OFDM, its advantage is that it does not use FFT or inverse FFT, but uses simple square-root raised cosine (SRRC) filter [11]. Moreover, the power efficiency is higher while the spectral efficiency remains similar [10].

$$g_{SRRC}(t) = \frac{2\alpha[cos(\frac{(1+\alpha)\pi t}{T_S}) + (\frac{4\alpha t}{T_S})^{-1} sin(\frac{(1-\alpha)\pi t}{T_S})]}{\pi\sqrt{T_S}[1-(\frac{4\alpha t}{T_S})^2]} \quad (1)$$

where, α is the filter roll-off factor, $T_s = 1/R_s$ is the symbol period, R_S is the system baud rate, and t is the instantaneous time sample.

III. Channel Measurement Campaign

In order to better realize the indoor OWC system, comprehensive channel characterization helps better understand the corresponding OWC channel, which is a necessary condition for designing a high-performance OWC system.

In our specific experimental scenario, to achieve integrated sensing and communication, our main idea is to replace the

existing wired communication link with a new optical wireless link. We exploit short links with a free line of sight (LOS) to multiple optical wireless access points mounted on the ceiling. The measurements are performed on the downlink. Assuming that the optical front end is reciprocal (i.e., has the same beam characteristics in uplink and downlink), the measurement data can also be used to characterize the uplink channel.

In this section, we provide details on our experimental setup in the lab, the measurement methodology, the Tx and Rx configurations considered for channel characterization, and the setup of an indoor OWC communication performance test using m-CAP modulation.

A. Experimental Setup

A network analyzer (ENA Network Analyzer, Agilent E5061B), connected between the optical Tx and Rx is used to measure the frequency responses for all Tx-Rx configurations of the communication system. Our Tx optical frontend consists of an IR LED powered by the driver circuit to deliver high optical power to the coverage area. At the Rx, three PDs are used to increase the total sensitive area and collect more optical power. This ensures a wide coverage area and enables mobile optical communication. In this experimental setup, by using the amplifier and attenuator, a gain of 13dB is provided for Tx, so that the transmitting signal reaches the maximum voltage that the device allows to receive ($V_{pp} \approx 3.4V$, V_{pp} of antenna's should be less than 6V.) This gain improves the detectability of the optical wireless signals in realistic scenarios [16].

B. Channel Response Calibration

Measurements are performed using the classical continuous wave (CW) frequency-sweep technique [17]. The Network Analyzer applied a CW signal of 0 dBm electrical power to the optical Tx, where the modulation frequency of the LED varies from 100 kHz to 200 MHz. Due to the bandwidth limitations in our frontend, we keep the maximum sweep frequency at 200 MHz. The Network Analyzer compares the amplitude and phase of the transmitted signal with the received signal and thereby delivers the frequency response of the device-under-test. In our case, the device-under-test comprises the wireless link and the optical frontends.

The measured overall frequency response of the system $H_{Sys}(f)$ is represented as:

$$H_{Sys}(f) = H_{Rx}(f) \cdot H_{Ch}(f) \cdot H_{Tx}(f) \tag{2}$$

where $H_{Rx}(f)$ is the frequency response of the Rx, $H_{Tx}(f)$ is the frequency response of the Tx and $H_{Ch}(f)$ represents the frequency response of the IR communication channel.

For characterizing the IR communication propagation channel, the impact of the frontends has to be removed [16]. Therefore, a calibration is performed by keeping the Tx and Rx at the reference LOS distance d_{ref} of 1 m. The reference distance d_{ref} is selected such that the link has negligible distortion, i.e. no signal clipping or saturation is observed at the receiver. The response of reference channel is given as:

$$H_{Ref}(f) = H_{Rx}(f) \cdot H_{d_{ref}}(f) \cdot H_{Tx}(f) \tag{3}$$

where $H_{d_{ref}}(f)$ is the frequency response of the LOS reference channel.

Correspondingly, a normalized frequency response of the IR communication channel is obtained as:

$$H_{Ch_{norm}}(f) = \frac{H_{Sys}(f)}{H_{Ref}(f)} = \frac{H_{Ch}(f)}{H_{d_{ref}}(f)} \tag{4}$$

Based on $H_{Ch_{norm}}(f)$, all other channel parameters such as channel impulse response (CIR), root-mean-square (RMS) delay spread, as well as path loss can be determined. In the remainder of this paper, we consider the channel response as the obtained data from equation (4), i.e., the impact of the optical frontends is always removed. Accordingly, the LOS reference channel response $H_{d_{ref}}(f)$ is represented by 0 dB in the amplitude response of the normalized IR communication channels.

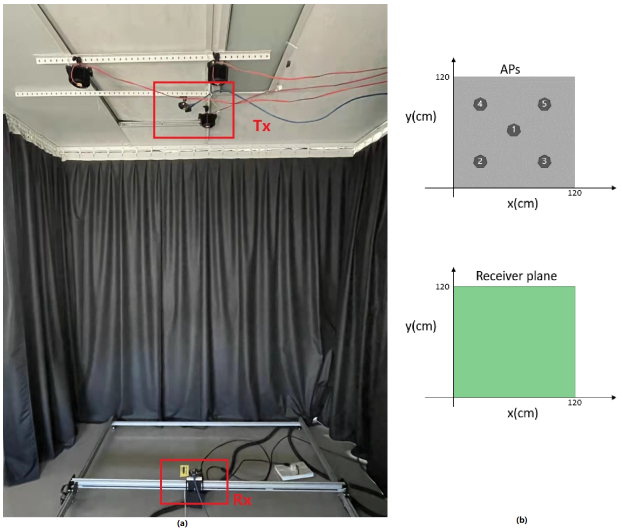

Fig. 3. Laboratory Setup. (a) The laboratory scenario, Tx and Rx positions are marked in red. (b) A diagram of the location of APs and the receiver plane

C. Tx-Rx Configurations

The considered LOS measurement and communication performance test scenario is shown in Fig.3. In this case, we investigated the performance of an IR communication system deployed in a laboratory test bench (dimensions 1.2m x 1.2m x 1.96m). Tx was placed successively at five different locations, AP1, AP2, AP3, AP4 and AP5, on the ceiling of the laboratory. Rx is placed in the receiving area (120cmx120cm) directly below the transmitting end, as shown in Fig.3. For each AP position, Rx performs receiving sampling in the receiving area with a step of 10cm, a total of 13x13=169 data sets. The exact positions of all optical frontends in the room are given in Table I. Typically, in the considered scenario, the LED is pointed at the floor and the receiver at the ceiling.

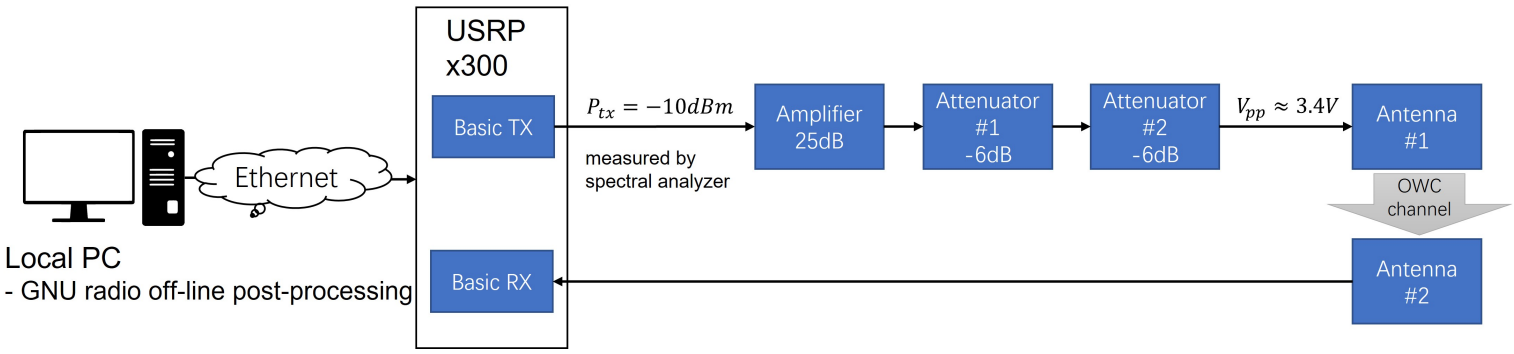

Fig. 4. Communication Performance Test System Diagram

TABLE I
POSITIONS OF TX AND RX FRONTENDS IN OUR EXPERIMENT

Optical frontends(OFE)	Positions in m(x,y,z)
AP1	(0.6,0.6,1.96)
AP2	(0.3,0.3,1.96)
AP3	(0.3,0.9,1.96)
AP4	(0.9,0.3,1.96)
AP5	(0.9,0.9,1.96)
Rx_{Ref}	(0.6,0.6,0.96)
Rx	(x,y,0)($0 \geq x \leq 1.2, 0 \geq y \leq 1.2$)

TABLE II
M-CAP PARAMETER SETTING

signalBandwidth	10e6
F_samp	20e6
rolloff	0.4
span	10
F_{sc}	$[1, 3, 5, 7] . * 10e6$
scBandwidth	1e6
QAM	16
n	10e5

D. Communication Performance Test Steps

Based on the settings in the previous section, procedure in the communication performance test, shown in Fig.4, we use the GNU Radio software platform on the Local PC to generate signal data and send it to USRP x300 through Ethernet to generate a Tx signal with an output power of -10dBm. Before going to the LED, a 25dB amplifier and two -6dB Attenuators pass through, so that V_{pp} increases to 3.4V close to the V_{pp} requirement. The signal is sent out by the IR LED and received by the PD, and finally the data is sent back to the Local PC via the USRP x300 for offline processing. The same test is performed for each AP location (listed in Table I), as follows:

1. Use the GNU Radio software platform to generate the m-CAP communication signal (m-CAP parameter setting see Table II) required for the test, and use the USRP X300 to send the signal to Tx.

2. For each AP, Rx receives signals with 10cm step distance in the receiving area, and a total of 13*13=169 groups of results are obtained for each group.

3. Calculate the BER and EVM of each group of received data separately

IV. MEASUREMENT RESULT AND ANALYSIS

This section reports and discusses the channel measurement results and communication test results for the various Tx-Rx configurations. The purpose is to provide basic insight into the characteristics of point-to-point channel characteristics and communication performance for the indoor OWC system research.

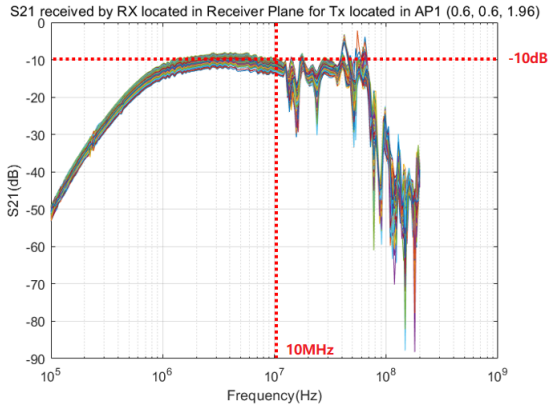

Fig. 5. $H_{Sys}(f)$: The measured overall frequency response of the system

A. Channel Response

The measured S21 (represents the power received at PD relative to the power input to LED here) responses of the LOS channel corresponding to Tx at the AP1 position, and Rx at all positions (given in Table I) are shown in Fig.5. It shows that the Tx device has stable performance at a frequency below 10M, and the attenuation is small (about 10dB). Therefore, since the S21 in this interval is stable and has the least attenuation, it is suitable for communication

The measured amplitude responses of the LOS channels corresponding to Tx at the AP1 position and Rx at all positions are shown in Fig.6. It can be seen from $H_{Ch_{norm}}(f)$ that the IR communication system performs well in the low frequency range under the LOS channel, and can obtain the signal sent

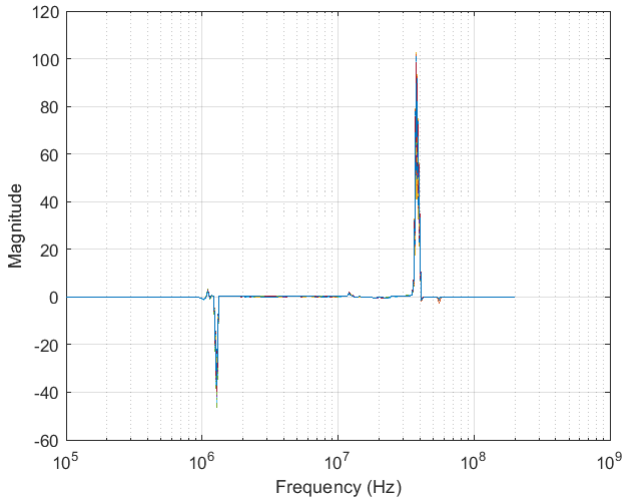

Fig. 6. $H_{Ch_{norm}}(f)$: Amplitude responses of IR channels in LOS configurations

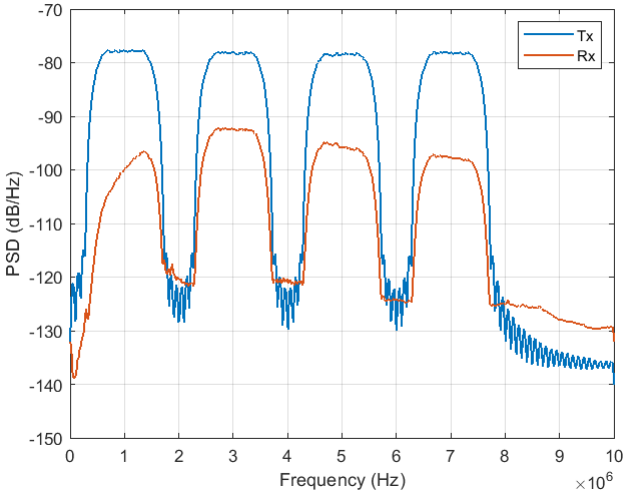

Fig. 8. Spectrum comparison of Tx and Rx signals

by the Tx end well in the frequency range from 1M to 30MHz. Among them, the two abrupt points appearing in the figure are caused by the fact that the amplitude of $H_{Ref}(f)$ (shown in Fig.7) as the denominator is close to 0 at these two places.

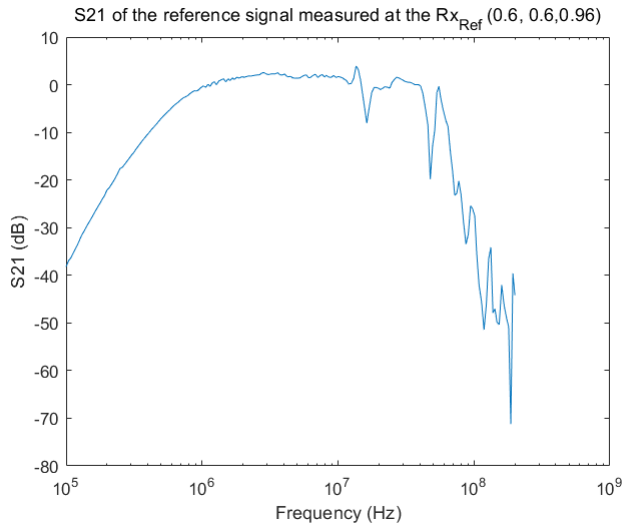

Fig. 7. $H_{Ref}(f)$: The response of reference channel

the performance of the first sub-CAP is slightly weaker than the other three sub-CAPs. Therefore, different sub-CAPs can be used to transmit different signal data for communication. According to the different Tx positions (given in Table I),

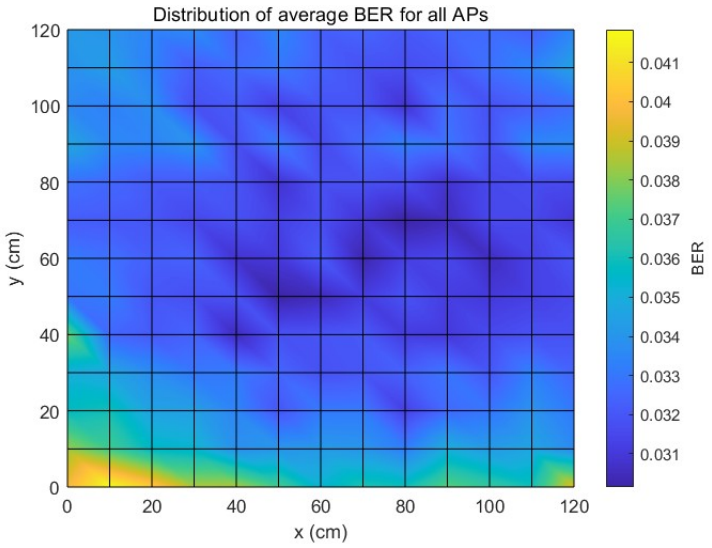

Fig. 9. Distribution of average BER for all Access Points

B. Communication Test Result

In this experimental environment, when Tx is located at a height of 1.96m, the Rx on the ground can receive signals that can be used for communication in the range of $0.9^2 * \pi \approx 2.54m^2$. Comparing the spectrum diagrams of the Tx signal and the Rx signal in Fig.8, it can be seen that the average amplitude of the Rx signal is about -107.2431dB and the average loss is about 13.5267dB. The average amplitudes of the four sub-CAPs are similar and stable. Because Tx has a large signal attenuation at low frequency (0-1MHz), there are five sets of experimental results of the communication tests. Fig.9 and Fig.10 show the average BER distribution and the average EVM distribution of the five sets of experiments results respectively. For the average BER distribution, the minimum value of BER is 0.0301, the maximum value is 0.0418, and the average value is 0.0330. Since the amplitude of the signal received in the central area is higher than that of the surrounding area, the performance of nearly 85% of the area near the center is relatively better. Similarly, for the average EVM distribution, the minimum value of EVM is 18.8338%, the maximum value is 24.8491%, and the average value is

20.6649%. The distribution also shows that the central area is better than the surrounding area. In addition, because the area where the coordinates are located on the side of y=0 is the connection of the shading cloth, affected by the external environment, when the position of Rx is close to the side of y=0, the performance of BER and EVM is slightly worse. It can be seen that the system can perform the communication work well in the laboratory environment. The result proves that the system can complete the communication task very well According to the DCSS issued by DCI [18] [19], the system meets the transmission standard of 4K radio.

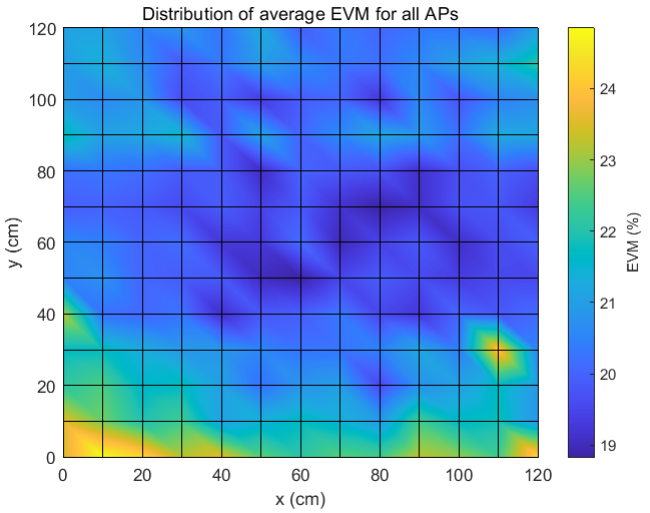

Fig. 10. Distribution of average EVM for all Access Points

V. CONCLUSIONS

In this paper, the indoor OWC channel measurement platform was successfully established, and the IR and photodiode device was used as the transceiver device, its channel characteristics have been successfully measured, and its communication performance was verified using the m-CAP modulation scheme. Through experiments, the channel response of the IR device is measured. In addition, according to the test results of communication performance, its four sub-CAPs are flat in the frequency domain, and the amplitude attenuation is small, so different sub-CAPs can be used to transmit different signal data for communication. The OWC channel measurement testbed can achieve a data rate above 16Mbps, with the minimum value of EVM 18.8338%, and the minimum value of BER 0.0301. According to the Digital Cinema System Specification issued by DCI, the system meets the transmission standard of 4K radio.

ACKNOWLEDGMENT

The authors gratefully acknowledge the financial supports of the Chinese Scholarship Council and the EU Horizon 2020 program towards the 6G BRAINS project H2020-ICT 101017226.

REFERENCES

[1] D. K. P. Tan, J. He, Y. Li, A. Bayesteh, Y. Chen, P. Zhu, and W. Tong, "Integrated sensing and communication in 6g: Motivations, use cases, requirements, challenges and future directions," in *2021 1st IEEE International Online Symposium on Joint Communications & Sensing (JC&S)*, pp. 1–6, IEEE, 2021.

[2] B. Dong, J. Jia, G. Li, J. Shi, H. Wang, J. Zhang, and N. Chi, "Demonstration of photonics-based flexible integration of sensing and communication with adaptive waveforms for a w-band fiber-wireless integrated network," *Optics Express*, vol. 30, no. 22, pp. 40936–40950, 2022.

[3] W. Saad, M. Bennis, and M. Chen, "A vision of 6g wireless systems: Applications, trends, technologies, and open research problems," *IEEE network*, vol. 34, no. 3, pp. 134–142, 2019.

[4] Y. Cui, F. Liu, X. Jing, and J. Mu, "Integrating sensing and communications for ubiquitous iot: Applications, trends, and challenges," *IEEE Network*, vol. 35, no. 5, pp. 158–167, 2021.

[5] X. You, C.-X. Wang, J. Huang, X. Gao, Z. Zhang, M. Wang, Y. Huang, C. Zhang, Y. Jiang, J. Wang, *et al.*, "Towards 6g wireless communication networks: Vision, enabling technologies, and new paradigm shifts," *Science China Information Sciences*, vol. 64, no. 1, pp. 1–74, 2021.

[6] M. Z. Chowdhury, M. Shahjalal, M. K. Hasan, and Y. M. Jang, "The role of optical wireless communication technologies in 5g/6g and iot solutions: Prospects, directions, and challenges," *Applied Sciences*, vol. 9, no. 20, p. 4367, 2019.

[7] M. Uysal and H. Nouri, "Optical wireless communications — an emerging technology," in *2014 16th International Conference on Transparent Optical Networks (ICTON)*, pp. 1–7, 2014.

[8] L. Grobe, A. Paraskevopoulos, J. Hilt, D. Schulz, F. Lassak, F. Hartlieb, C. Kottke, V. Jungnickel, and K.-D. Langer, "High-speed visible light communication systems," *IEEE communications magazine*, vol. 51, no. 12, pp. 60–66, 2013.

[9] D. Tsonev, H. Chun, S. Rajbhandari, J. J. McKendry, S. Videv, E. Gu, M. Haji, S. Watson, A. E. Kelly, G. Faulkner, *et al.*, "A 3-gb/s single-led ofdm-based wireless vlc link using a gallium nitride μ led," *IEEE photonics technology letters*, vol. 26, no. 7, pp. 637–640, 2014.

[10] F. M. Wu, C. T. Lin, C. C. Wei, C. W. Chen, Z. Y. Chen, H. T. Huang, and S. Chi, "Performance comparison of ofdm signal and cap signal over high capacity rgb-led-based wdm visible light communication," *IEEE Photonics Journal*, vol. 5, no. 4, pp. 7901507–7901507, 2013.

[11] M. M. Merah, *Conception and realization of an indoor multi-user Light-Fidelity link*. PhD thesis, Université Paris-Saclay, 2019.

[12] P. A. Haigh, P. Chvojka, S. Zvanovec, Z. Ghassemlooy, S. T. Le, T. Kanesan, E. Giacoumidis, N. J. Doran, I. Papakonstantinou, and I. Darwazeh, "Experimental verification of visible light communications based on multi-band cap modulation," in *Optical Fiber Communication Conference*, pp. Tu2G–2, Optica Publishing Group, 2015.

[13] T. Collins and H. Bidgoli, "Carrierless amplitude phase modulation," in *The Handbook of Computer Networks*, 2007.

[14] M. I. Olmedo, T. Zuo, J. B. Jensen, Q. Zhong, X. Xu, S. Popov, and I. T. Monroy, "Multiband carrierless amplitude phase modulation for high capacity optical data links," *Journal of Lightwave Technology*, vol. 32, no. 4, pp. 798–804, 2013.

[15] P. A. Haigh, S. T. Le, S. Zvanovec, Z. Ghassemlooy, P. Luo, T. Xu, P. Chvojka, T. Kanesan, E. Giacoumidis, P. Canyelles-Pericas, *et al.*, "Multi-band carrier-less amplitude and phase modulation for bandlimited visible light communications systems," *IEEE Wireless Communications*, vol. 22, no. 2, pp. 46–53, 2015.

[16] S. M. Mana, P. Hellwig, J. Hilt, P. W. Berenguer, and V. Jungnickel, "Experiments in non-line-of-sight li-fi channels," in *2019 Global LIFI Congress (GLC)*, pp. 1–6, IEEE, 2019.

[17] J. M. Kahn and J. R. Barry, "Wireless infrared communications," *Proceedings of the IEEE*, vol. 85, no. 2, pp. 265–298, 1997.

[18] DCI, *Digital Cinema System Specifications v1.4.1*. Digital Cinema Initiatives, LLC, 2021.

[19] "Internet connection speed recommendations." https://help.netflix.com/en/node/306, 2014.